

Supporting Information

Stable Bioelectric Signal Acquisition using Enlarged-Surface-Area Flexible Skin Electrode

Inyeol Yun,^a Jinpyeo Jeung,^a Hyungsub Lim,^b Jieun Kang,^c Sangyeop Lee,^c

Seongmin Park,^a Suwon Seong,^a Soojin Park,^c Kilwon Cho,^b and Yoonyoung

Chung^{a,d,}*

^a Department of Electrical Engineering, Pohang University of Science and
Technology, Pohang, Gyeongbuk 37673, Korea

^b Department of Chemical Engineering, Pohang University of Science and
Technology, Pohang, Gyeongbuk 37673, Korea

^c Department of Chemistry, Pohang University of Science and Technology, Pohang,
Gyeongbuk 37673, Korea

^d Center for Semiconductor Technology Convergence, Pohang University of Science

and Technology, Pohang, Gyeongbuk 37673, Korea

* E-mail: ychung@postech.ac.kr

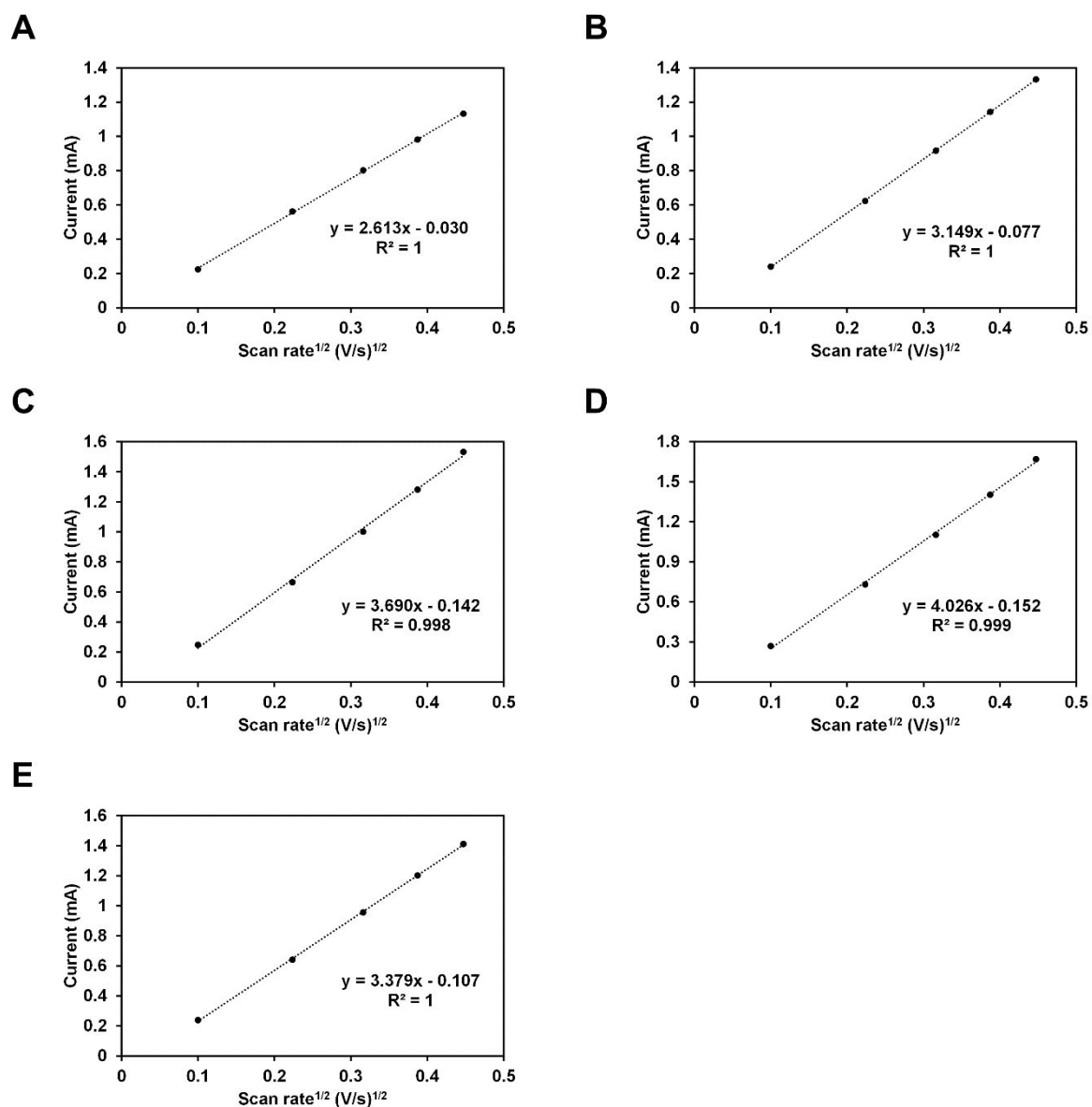


Figure S1. Peak current data from cyclic voltammetry measurements on electrodeposited Au

electrode as a function of the square root of scan rate. The concentration of HAuCl_4 in electrodeposition solution was fixed at 3 mM, and the deposition time was varied at A) 0 sec, B) 30 secs, C) 60 secs, D) 90 secs, E) 120 secs.

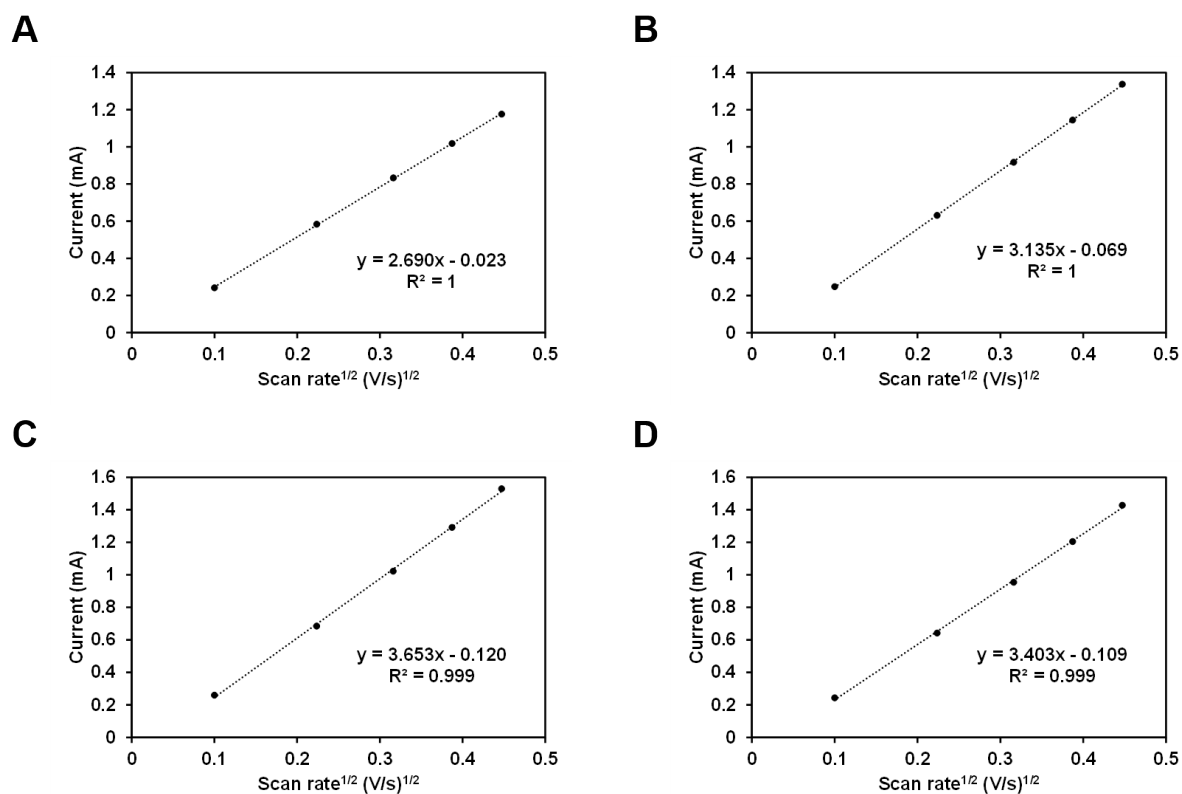


Figure S2. Peak current data from cyclic voltammetry measurements on electrodeposited Au electrode as a function of the square root of scan rate. The deposition time was fixed at 90 secs, and the concentration of H[AuCl₄] solution was varied at A) 1 mM, B) 2 mM, C) 4 mM, D) 5 mM.

Electrode Surface Area Calculation

Electrically active surface area was calculated using the Randles-Sevcik equation:

$$i_p = 2.69 \times 10^5 \cdot n^{\frac{3}{2}} \cdot A \cdot D^{\frac{1}{2}} \cdot C \cdot v^{\frac{1}{2}},$$

where i_p is the peak current of the cyclic voltammetry (CV) measurement, n is the number of electrons transferred in the redox reaction, A is the area of the electrode, D is the diffusion coefficient, C is the concentration of electrochemical redox pair in the solution and v is the scan rate.

CV measurements were performed on bare Au and ESASE in various scan rate (see **Figure S2**). The peak current was plotted as a function of the square root of scan rate in **Figure S3** for the surface area calculation. n is 1 with $\text{Fe}(\text{CN})_6$ solution, and D is $6.67 \times 10^{-6} \text{ cm}^2\text{s}^{-1}$ from a previous study^{S1}. The calculated surface area of each electrode is shown in **Table 1** of the main text.

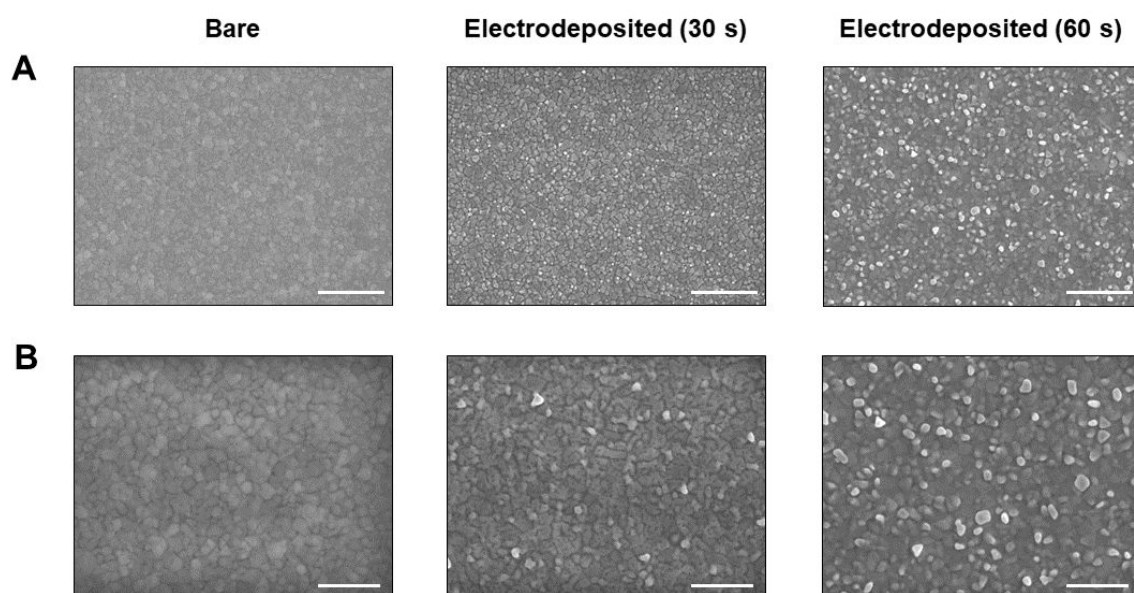


Figure S3. Morphology characterization of bare and electrodeposited gold electrodes. The time denotes the processing time for electrodeposition. A) Low (scale bar: 1 μm) and B) high (scale bar: 500 nm) magnification SEM images. The size and the number of gold nanoparticles were increased in electrochemical deposition.

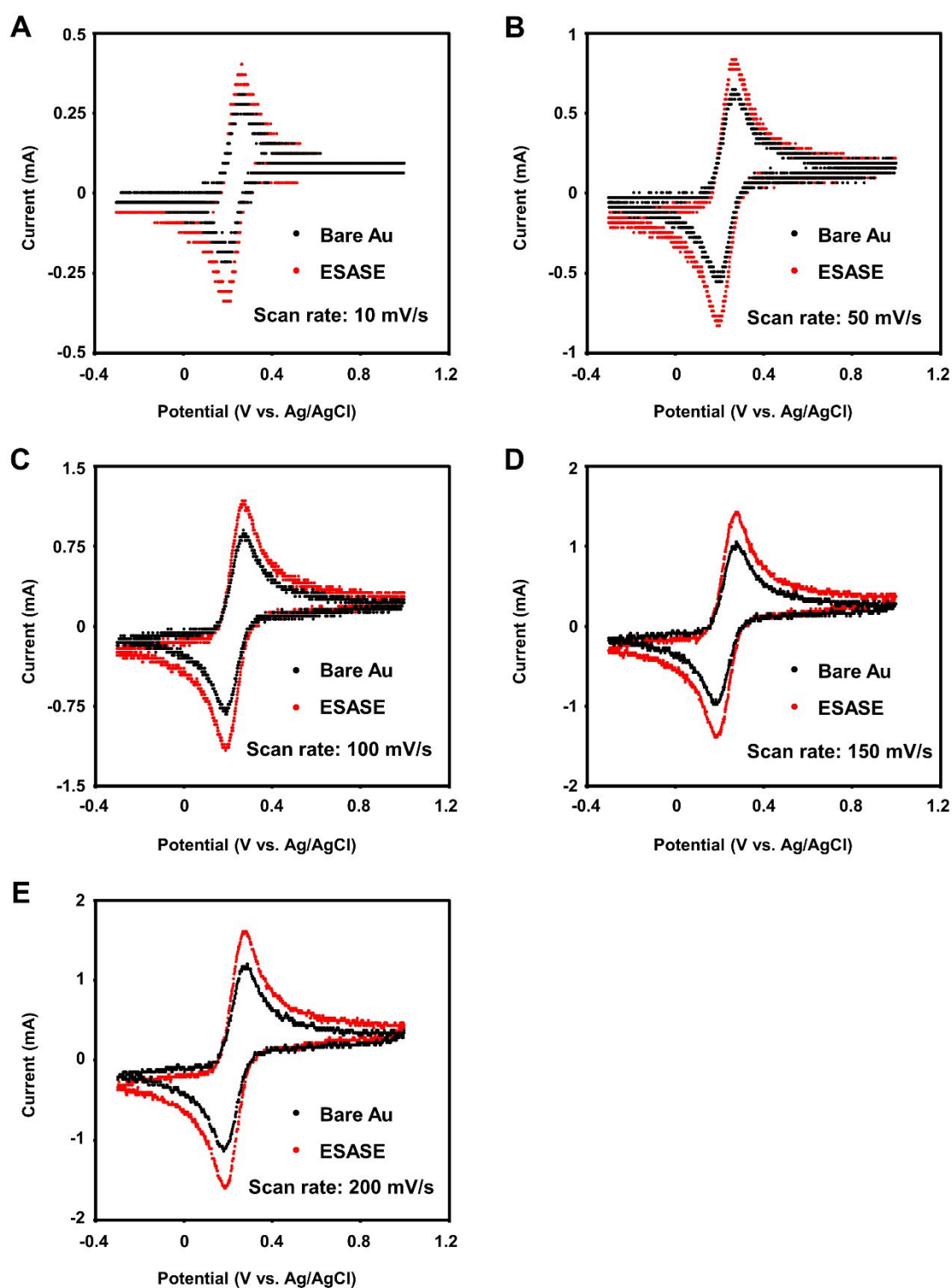


Figure S4. Cyclic voltammetry data of bare Au and ESASE with potential scan rate of A) 10 mV/s, B) 50 mV/s, C) 100 mV/s, D) 150 mV/s and E) 200 mV/s.

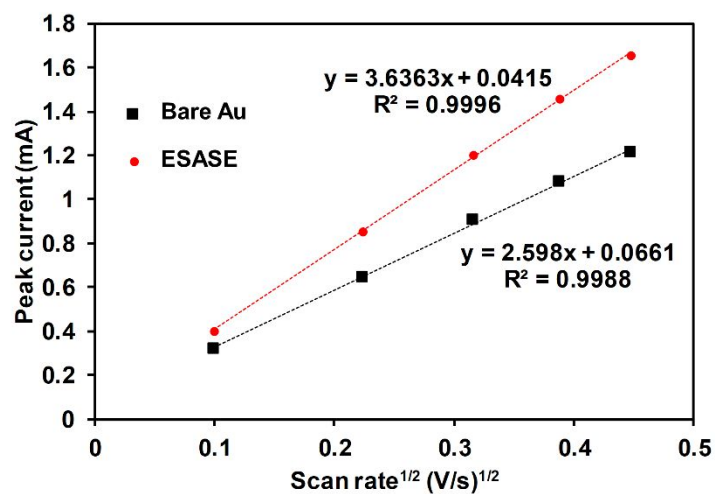


Figure S5. Peak current data from cyclic voltammetry measurements as a function of the square root of scan rate. The regression line of the ESASE exhibits a larger slope than the bare Au, indicating an increased surface area. The surface area of ESASE is 40% larger than that of the bare Au.

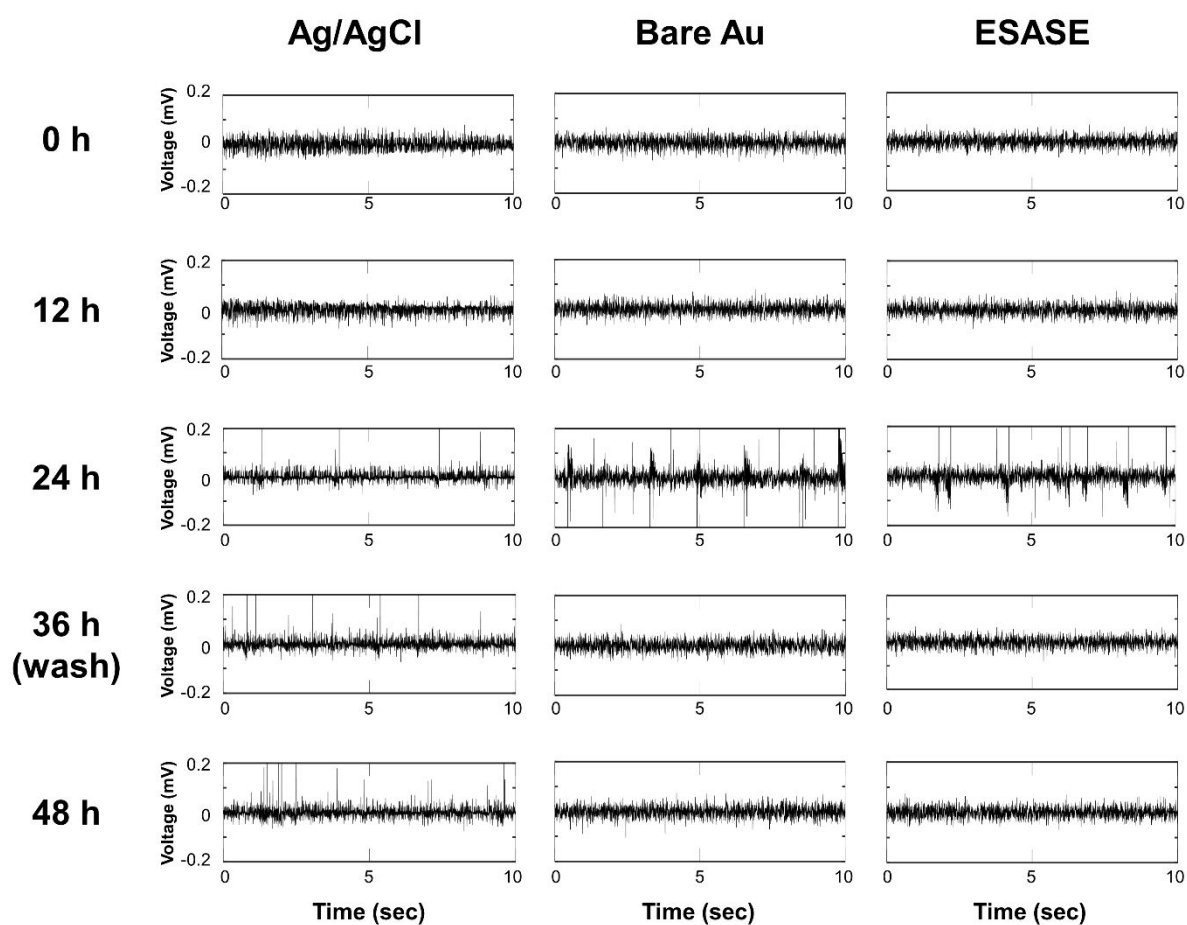


Figure S6. Thermal noise measurement (0–48 hours) using the three types of electrodes: Ag/AgCl, bare Au and ESASE. Spasmodic noise peaks increase over time. After cleaning the electrode surface with distilled water at 36 hours, the noise spike from bare Au and ESASE was disappeared, but the Ag/AgCl electrode was not recovered due to the chemical byproducts strongly attached onto the surface.

Table S1. Standard deviation (SD) and its ascending rank (R) of muscle fatigue indicators, MNF and MDF, for each subject and workout. The muscle fatigue indicators were extracted from the measured EMG signal after each workout. The ESASE exhibits the lowest variation in most data.

		Ag/AgCl, SD (R)	Bare Au, SD (R)	ESASE, SD (R)
Subject 1	MNF	Workout 1	1.99 (3)	1.84 (2)
		Workout 2	2.44 (3)	1.93 (2)
		Workout 3	1.61 (2)	3.06 (3)
		Workout 4	1.53 (2)	2.36 (3)
		Workout 5	2.29 (2)	3.14 (3)
		Workout 6	2.04 (3)	1.08 (1)
	MDF	Workout 1	2.60 (2)	2.65 (3)
		Workout 2	3.64 (3)	3.08 (2)
		Workout 3	3.13 (2)	5.09 (3)
		Workout 4	2.64 (2)	2.85 (3)
		Workout 5	3.33 (2)	3.92 (3)
		Workout 6	3.21 (3)	2.15 (2)
Subject 2	MNF	Workout 1	1.19 (2)	1.45 (3)
		Workout 2	1.15 (3)	0.76 (1)
		Workout 3	1.22 (2)	1.18 (1)
		Workout 4	0.78 (1)	1.50 (2)
		Workout 5	1.17 (2)	0.63 (1)
		Workout 6	1.23 (2)	1.96 (3)
	MDF	Workout 1	1.01 (2)	4.06 (3)
		Workout 2	1.56 (2)	1.75 (3)
		Workout 3	2.11 (2)	3.35 (3)
		Workout 4	1.12 (2)	1.62 (3)
		Workout 5	1.69 (2)	1.70 (3)
		Workout 6	1.07 (2)	3.97 (3)
Subject 3	MNF	Workout 1	2.10 (3)	1.05 (1)
		Workout 2	1.67 (3)	0.35 (1)
		Workout 3	1.34 (1)	2.31 (3)
		Workout 4	1.44 (3)	1.38 (2)
		Workout 5	0.93 (1)	2.59 (3)

Subject 4	MDF	Workout 6	0.52 (1)	1.40 (3)	1.38 (2)
		Workout 1	3.16 (3)	1.18 (1)	2.00 (2)
		Workout 2	2.09 (3)	0.57 (1)	1.38 (2)
		Workout 3	2.94 (2)	2.95 (3)	1.90 (1)
		Workout 4	2.72 (3)	1.46 (2)	0.34 (1)
		Workout 5	1.14 (1)	2.97 (3)	1.75 (2)
		Workout 6	1.70 (2)	1.98 (3)	0.52 (1)
	MNF	Workout 1	1.31 (2)	1.42 (3)	1.11 (1)
		Workout 2	2.40 (3)	1.42 (1)	1.81 (2)
		Workout 3	0.65 (1)	1.20 (3)	1.19 (2)
		Workout 4	1.83 (3)	0.82 (1)	1.48 (2)
		Workout 5	3.58 (3)	1.23 (2)	0.92 (1)
		Workout 6	2.01 (3)	1.14 (2)	0.59 (1)
Subject 5	MDF	Workout 1	2.28 (3)	1.71 (2)	1.26 (1)
		Workout 2	3.56 (3)	1.04 (1)	2.67 (2)
		Workout 3	3.65 (3)	1.03 (1)	1.26 (2)
		Workout 4	3.07 (3)	2.50 (1)	2.86 (2)
		Workout 5	5.73 (3)	1.03 (1)	2.02 (2)
		Workout 6	3.05 (3)	1.69 (2)	1.60 (1)
	MNF	Workout 1	4.55 (3)	0.66 (2)	0.30 (1)
		Workout 2	2.64 (3)	1.23 (2)	1.04 (1)
		Workout 3	1.14 (2)	1.00 (1)	1.15 (3)
		Workout 4	2.62 (3)	0.85 (2)	0.50 (1)
		Workout 5	1.10 (2)	3.21 (3)	0.70 (1)
		Workout 6	1.03 (2)	1.75 (3)	0.76 (1)
Subject 6	MDF	Workout 1	4.43 (3)	2.13 (2)	1.44 (1)
		Workout 2	2.92 (3)	1.84 (2)	1.66 (1)
		Workout 3	2.15 (2)	1.82 (1)	2.57 (3)
		Workout 4	3.62 (3)	1.60 (1)	1.61 (2)
		Workout 5	1.81 (2)	6.03 (3)	1.24 (1)
		Workout 6	0.46 (1)	2.48 (3)	1.70 (2)
	MNF	Workout 1	1.10 (2)	0.90 (1)	1.34 (3)
		Workout 2	2.54 (3)	0.77 (1)	1.44 (2)
		Workout 3	0.73 (1)	2.30 (3)	1.58 (2)
		Workout 4	1.44 (2)	1.59 (3)	1.15 (1)
		Workout 5	0.56 (1)	1.66 (3)	1.44 (2)
		Workout 6	0.91 (1)	2.56 (3)	0.94 (2)
	MDF	Workout 1	1.68 (3)	0.97 (1)	1.39 (2)
		Workout 2	3.57 (3)	1.18 (1)	2.18 (2)
		Workout 3	1.32 (1)	2.86 (3)	1.93 (2)

Subject 7	MNF	Workout 4	2.62 (3)	2.48 (2)	1.12 (1)
		Workout 5	1.41 (2)	2.55 (3)	1.03 (1)
		Workout 6	1.17 (2)	2.65 (3)	0.61 (1)
		Workout 1	2.34 (3)	2.22 (2)	1.59 (1)
		Workout 2	3.41 (3)	0.99 (1)	1.03 (2)
		Workout 3	0.91 (1)	2.44 (3)	1.90 (2)
	MDF	Workout 4	0.95 (1)	1.11 (2)	2.11 (3)
		Workout 5	2.95 (3)	0.77 (2)	0.41 (1)
		Workout 6	2.05 (3)	1.58 (2)	0.65 (1)
		Workout 1	1.48 (1)	3.67 (2)	4.04 (3)
		Workout 2	4.74 (3)	2.24 (2)	1.38 (1)
		Workout 3	1.98 (2)	3.07 (3)	1.14 (1)
Subject 8	MNF	Workout 4	2.37 (3)	1.74 (1)	2.24 (2)
		Workout 5	5.39 (3)	1.72 (2)	1.04 (1)
		Workout 6	2.91 (3)	2.08 (2)	1.47 (1)
		Workout 1	0.57 (1)	1.42 (3)	0.67 (2)
		Workout 2	0.85 (1)	1.03 (2)	1.10 (3)
		Workout 3	1.64 (3)	0.78 (1)	0.84 (2)
	MDF	Workout 4	1.01 (1)	2.42 (3)	1.36 (2)
		Workout 5	0.85 (1)	1.41 (3)	0.91 (2)
		Workout 6	1.22 (3)	1.01 (2)	0.76 (1)
		Workout 1	1.16 (3)	1.01 (2)	0.62 (1)
		Workout 2	1.07 (2)	0.67 (1)	1.26 (3)
		Workout 3	1.73 (3)	0.56 (1)	1.46 (2)
Average	Workout 4	1.20 (1)	1.30 (2)	1.38 (3)	
	Workout 5	1.46 (3)	1.35 (1)	1.41 (2)	
	Workout 6	2.17 (2)	2.72 (3)	0.57 (1)	
		2.03 (2.27)	1.87 (2.13)	1.30 (1.58)	

Supplementary Reference

S1 Ameer, Z. O.; Husein, M. M. Electrochemical behavior of potassium ferricyanide in aqueous and (w/o) microemulsion systems in the presence of dispersed nickel nanoparticles. *Sep. Sci Technol.* **2013**, 48 (5), 681-689.